



## Egyptian Journal of Biophysics and Biomedical Engineering

<https://ejbbe.journals.ekb.eg/>

### Investigate the Biophysical-Biochemical Properties of (Chitosan - Polyacrylic Acid) Nanogel Loaded Berberine for use in Biomedical Application

Mohamed. I. Meligy <sup>1\*</sup>, Mahmoud H. Abdelgawad <sup>1</sup>, Shaimaa M. Nasef <sup>2</sup> and H.H. El-Bahnasawy <sup>1</sup>



CrossMark

<sup>1</sup>Physics Department, Faculty of Science, Al-Azhar University, Nasr City, 11884, Cairo, Egypt.

<sup>2</sup>Polymer Chemistry Dep., National Center for Radiation Research and Technology, Egyptian Atomic Energy Authority, P.O. Box 29, Cairo, Egypt.

**T**HE moist and nutrient-rich environment of skin wounds creates an ideal setting for the proliferation of microorganisms, which can impede the natural healing process. Conventional treatments, such as antimicrobial creams, often suffer from inconsistent dosing, limiting their efficacy. This study explores the potential of a chitosan/poly(acrylic acid) (Cs/PAA) nanogel loaded with berberine to enhance bioavailability and anti-inflammatory properties, thereby promoting wound healing. The nanogel was synthesized through gamma radiation-induced polymerization of acrylic acid in a chitosan aqueous solution. The resulting nanogels were characterized using advanced techniques, including Transmission Electron Microscopy (TEM) for morphological analysis, Dynamic Light Scattering (DLS) for particle size distribution, Zeta potential for surface charge determination, and Thermogravimetric Analysis (TGA) for thermal stability assessment. Additionally, the wound-healing potential was evaluated using fibroblast cell lines. The findings revealed that the berberine-loaded Cs/PAA nanogel exhibited significantly improved bioavailability, antimicrobial activity, and apoptotic effects compared to the berberine-free Cs/PAA nanogel. **Conclusions**, these results suggest that the berberine-loaded Cs/PAA nanogel represents a novel and promising therapeutic strategy for the effective treatment of skin wounds, offering enhanced therapeutic outcomes through optimized drug delivery and biological activity.

**Keywords:** Gamma irradiation, Chitosan/Polyacrylic Nanogel, Berberine, , anti-microbial, Wound healing.

### Introduction

The increasing prevalence of skin wounds and infections, coupled with the growing demand for natural, effective, and sustainable wound healing therapies, has made wound management a critical challenge in healthcare. When the dermal layer is exposed to the environment due to injury or pathogenic invasion, rapid healing is essential to restore skin integrity. The wound healing process is a complex, dynamic sequence involving four overlapping phases: hemostasis, inflammation, proliferation, and remodeling [1], [2]. In recent years, biopolymers have emerged as a pivotal class of materials in biomedical research due to their inherent flexibility, biodegradability, and biocompatibility, making them highly suitable for a wide range of therapeutic applications [3], [4].

Nanogels and microgels are colloidal networks composed of cross-linked polymer chains at the nano- or microscale, typically dispersed in aqueous solutions. Microgels are generally spherical particles with diameters ranging from 50 nm to 10  $\mu$ m, while nanogels are specifically defined as microgels with submicron dimensions [5]. Nanogels combine the advantages of nanoparticulate systems with the unique properties of hydrogels, such as hydrophilicity, flexibility, high water absorption capacity, and biocompatibility [6]. Compared to macro- and micro-scale drug delivery systems, nanogels offer superior benefits, including prolonged circulation times, reduced macrophage uptake, enhanced tissue penetration through biological membranes, and improved cellular recognition. These properties enable sustained therapeutic effects at the target site, with controlled release mechanisms that can last for days or even weeks [7].

The synthesis of microgels and nanogels often involves chemical cross-linking of natural or synthetic polymers through irradiation. During irradiation, water molecules absorb energy, leading to the formation of reactive species such as hydroxyl radicals, hydrogen radicals, solvated electrons, and hydrogen peroxide. These reactive intermediates interact with polymer chains, generating unpaired radicals that can recombine to form cross-linked networks. The outcome of irradiation—whether cross-linking or polymer degradation—depends on factors such as the polymer's chemical structure, molar mass, concentration, and irradiation conditions [8], [9]. Gamma radiation has become a widely used method for modifying polymer structures, initiating polymerization, grafting, sterilization, and cross-linking thermoplastics and elastomers. Its applications extend to high-performance fields

\*Corresponding author e-mail: meligy1991@gmail.com

Received: 21/03/2025; Accepted: 04/05/2025

DOI: 10.21608/EJB.2025.370164.1083

©2025 National Information and Documentation Center (NIDOC)

such as packaging, automotive, and electronics, where radiation-induced innovations have demonstrated significant commercial potential [10], [11].

Chitosan (CS), a natural polysaccharide derived from the deacetylation of chitin, is abundantly found in crustacean shells. Discovered in the 19th century, CS has gained prominence in biomedical and drug delivery applications over the past two decades due to its unique properties. Its hydrophilic and cationic nature enables interactions with negatively charged polymers or macromolecules, making it an ideal candidate for formulating nanohydrogels. Additionally, CS's mucoadhesive properties and stimuli-responsive behavior further enhance its suitability for advanced drug delivery systems [12].

Polyacrylic acid (PAA), a synthetic polymer derived from acrylic acid, is an anionic polymer that ionizes at neutral pH, conferring a negative charge. This property allows PAA to absorb and retain large amounts of water, swelling significantly beyond its original volume. PAA is widely used as a thickener, dispersant, suspending agent, and emulsifier in pharmaceuticals, cosmetics, and paints. Neutralized PAA gels are particularly valuable for creating biocompatible matrices in medical applications, such as skin care and wound treatment gels [13].

Berberine (BR), a naturally occurring alkaloid, has been used in traditional Chinese medicine for its anticancer and antibiotic properties [14], [15]. Its diverse pharmacological effects, including antioxidant, anti-inflammatory, antibacterial, antiviral, and hepatoprotective activities, make it a promising candidate for pharmaceutical development [16], [17]. However, BR's therapeutic potential is limited by its poor bioavailability, attributed to low solubility, inadequate tissue uptake, rapid metabolism, and elimination [18].

In this context, the present study aims to explore the therapeutic efficacy of berberine in wound healing by incorporating it into a chitosan-polyacrylic acid (Cs-PAA) nanogel matrix synthesized via gamma irradiation. The berberine-loaded nanogel was characterized using advanced techniques such as transmission electron microscopy (TEM), dynamic light scattering (DLS) for hydrodynamic diameter measurement, zeta potential analysis, and thermogravimetric analysis (TGA). Additionally, its bioavailability, antimicrobial activity, and wound healing potential were evaluated *in vitro* using fibroblast cell lines. This innovative formulation represents a promising approach to enhancing wound healing through improved drug delivery and therapeutic efficacy.

## **Material and methods**

### **Materials**

The chemicals utilized in this investigation comprised chitosan (Cs), a biopolymer with a molecular weight ranging from 100 to 300 kDa, sourced from Sigma-Aldrich (New Jersey, USA). Polyacrylic acid (PAA) was procured from Merck (Germany), whereas phosphate buffer solution (pH 7.4) and glacial acetic acid were supplied by El-Nasr Pharmaceutical Chemicals (Egypt). Additionally, berberine (BR) was acquired from Tokyo Chemical Industry (Tokyo, Japan). This selection of chemicals was essential for ensuring the reproducibility and consistency of experimental procedures, as each component plays a critical role in the physicochemical interactions under study.

### **Method of preparation**

#### **Preparation of (Cs / PAA) nanogel using gamma irradiation**

Chitosan/polyacrylic acid (Cs/PAA) nanogels were synthesized using a gamma irradiation technique, which promotes the polymerization and grafting of polyacrylic acid onto chitosan in solution [19]. The procedure involved dissolving 2 g of chitosan in 100 mL of a 1% (v/v) glacial acetic acid aqueous solution at 80°C for 2 hours, followed by the addition of 2 mL of polyacrylic acid (PAA) to prepare a 2% (w/v) chitosan - polyacrylic acid solution [20]. The resulting homogeneous mixture was subjected to gamma irradiation at the National Center for Radiation Research and Technology (Cairo, Egypt) using a Co-60 gamma cell facility. The irradiation was conducted at doses ranging from 2 to 50 kGy, with a dose rate of 0.814 kGy/h. This process facilitated the covalent grafting of polyacrylic acid onto the chitosan backbone, leading to the formation of nanogels with a well-defined structure and enhanced stability.

#### **Loading of Berberine onto Chitosan/Polyacrylic Acid Nanogels**

To load berberine into the Cs/PAA nanogels, 900 mg of berberine was dissolved in 100 mL of the Cs/PAA nanogel solution. The mixture was continuously stirred for 48 hours to ensure complete dissolution and uniform distribution of berberine within the nanogel matrix. Subsequently, the solution was processed using a spray dryer at an inlet temperature of 142°C to produce a dried nanogel powder loaded with berberine. This method ensured efficient encapsulation of Berberine within the nanogel structure, enhancing its potential for controlled release and therapeutic applications.

## Characterization of (chitosan/poly acrylic acid) nanogel

### Transmission electron microscopy (TEM)

The particle size and morphological characteristics of the chitosan/polyacrylic acid (Cs/PAA) nanogels were analyzed using a transmission electron microscope (TEM) (JEOL, JEM100CS, Japan) operating at an acceleration voltage of 80 kV. For imaging, the nanogel samples were appropriately diluted, deposited onto carbon-coated gold grids, and allowed to dry at ambient temperature. This approach enabled high-resolution visualization of the nanogel structure, providing critical insights into their size distribution, surface morphology, and overall uniformity, which are essential parameters for evaluating their potential applications in drug delivery and other biomedical fields.

### Particle Size and Zeta Potential Analysis

To evaluate the particle size and zeta potential, 2 mg of the sample was dispersed in 1 mL of deionized water and subjected to sonication for 5 minutes, followed by vortexing for 3 minutes to ensure uniform dispersion prior to measurements. The particle size and size distribution, expressed as average volume diameters and polydispersity index (PDI), were determined using photon correlation spectroscopy via a Dynamic Light Scattering (DLS) instrument (Zetasizer Nano ZN, Malvern Panalytical Ltd, United Kingdom). Measurements were conducted at a fixed scattering angle of 173° and a temperature of 25°C. Each sample was analyzed in triplicate to ensure reproducibility and accuracy. Additionally, the zeta potential, which reflects the surface charge and colloidal stability of the particles, was measured using the same instrument under identical conditions. These analyses provide critical insights into the physicochemical properties of the particles, which are essential for understanding their behavior in suspension and their potential applications in drug delivery systems.

### Thermogravimetric Analysis (TGA)

To evaluate the particle size and zeta potential, 2 mg of the sample was dispersed in 1 mL of deionized water and subjected to sonication for 5 minutes, followed by vortexing for 3 minutes to ensure uniform dispersion prior to measurements. The particle size and size distribution, expressed as average volume diameters and polydispersity index (PDI), were determined using photon correlation spectroscopy via a Dynamic Light Scattering (DLS) instrument (Zetasizer Nano ZN, Malvern Panalytical Ltd, United Kingdom). Measurements were conducted at a fixed scattering angle of 173° and a temperature of 25°C. Each sample was analyzed in triplicate to ensure reproducibility and accuracy. Additionally, the zeta potential, which reflects the surface charge and colloidal stability of the particles, was measured using the same instrument under identical conditions. These analyses provide critical insights into the physicochemical properties of the particles, which are essential for understanding their behavior in suspension and their potential applications in drug delivery systems.

### In Vitro Cell Viability Assessment

**Cell Culture,** The RAW264.7 mouse macrophage cell line was procured from Nawah Scientific Inc. (Mokatam, Cairo, Egypt). The cells were cultured in Dulbecco's Modified Eagle Medium (DMEM), supplemented with 100 µg/mL streptomycin, 100 units/mL penicillin, and 10% heat-inactivated fetal bovine serum (FBS). The cells were maintained under standardized conditions in a humidified incubator at 37°C with 5% (v/v) CO<sub>2</sub> to ensure optimal growth and viability.

**Cytotoxicity Assay,** Cell viability was evaluated using the Sulforhodamine B (SRB) assay, a well-established method for quantifying cell proliferation and cytotoxicity. Briefly, 100 µL aliquots of cell suspension, containing  $5 \times 10^3$  cells, were seeded into 96-well plates and incubated in complete media for 24 hours to allow cell attachment. Following incubation, the cells were treated with 100 µL of media containing the test drug at varying concentrations. After 72 hours of drug exposure, the cells were fixed by replacing the media with 150 µL of 10% trichloroacetic acid (TCA) and incubated at 4°C for 1 hour. The TCA solution was subsequently removed, and the cells were washed five times with distilled water to eliminate residual TCA.

Next, 70 µL of SRB solution (0.4% w/v) was added to each well, and the plates were incubated in the dark at room temperature for 10 minutes to allow SRB binding to cellular proteins. Unbound SRB was removed by washing the plates three times with 1% acetic acid, followed by air-drying overnight. Finally, 150 µL of 10 mM Tris base solution was added to each well to solubilize the protein-bound SRB stain. The absorbance of the resulting solution was measured at 540 nm using a BMG LABTECH® FLUOstar Omega microplate reader (Ortenberg, Germany) to quantify cell viability. This method provides a reliable and reproducible measure of cytotoxicity, enabling accurate assessment of drug effects on cellular proliferation and survival.

## Results and discussion

### Transmission Electron Microscopy (TEM) Analysis

As depicted in Figure 1, TEM micrographs revealed that both berberine (BR)-loaded and unloaded nanogel particles exhibited a spherical morphology with smooth surfaces [21]. The average diameter of the drug-unloaded nanogel particles was approximately 25 nm as shown in figure (1a), while the BR-loaded nanogel

particles showed an increased diameter of approximately 60 nm as shown in figure (1b). This size variation is likely attributed to the successful encapsulation of berberine within the chitosan (Cs)/polyacrylic acid (PAA) nanogel matrix[22]. Notably, both the drug-loaded and unloaded nanogel particles demonstrated minimal agglomeration, a critical characteristic for biomedical applications, particularly in drug delivery systems.

The absence of significant particle aggregation is a highly desirable feature, as it ensures a uniform dispersion of nanoparticles within the nanogel matrix [23]. This uniformity enhances the stability and bioavailability of the nanoparticles, facilitating prolonged contact time with the target site. Such properties are particularly advantageous for topical applications, as they promote the sustained release and enhanced penetration of berberine across the skin surface and into deeper wound tissues. These findings underscore the potential of Cs/PAA nanogels as an effective carrier for berberine, offering improved therapeutic efficacy in wound healing and other dermatological applications.

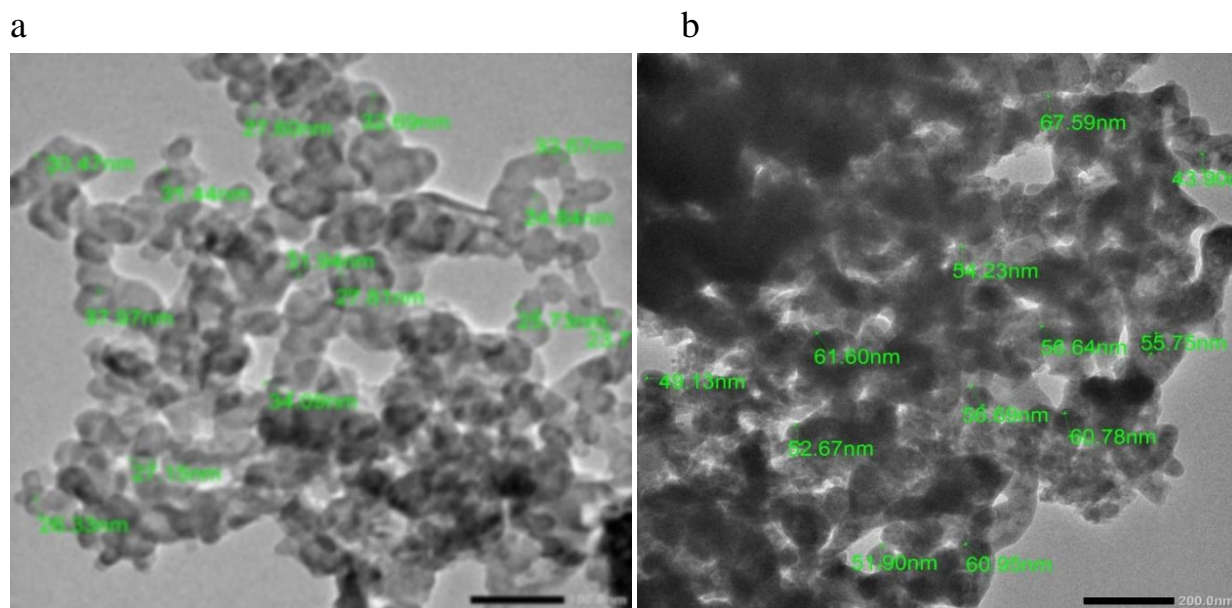


**Fig. 1** Transmission electron microscopy images of (a) Cs/PAA nanogel without BR, and (b) Cs/PAA nanogel loading BR.

#### Particle Size and Zeta Potential Analysis

The hydrodynamic radius and size distribution of the prepared chitosan (Cs)/polyacrylic acid (PAA) nanogels were evaluated using the Dynamic Light Scattering (DLS) technique, as summarized in Table 1. The DLS measurements provide insights into the swelling behavior of the nanogels, which is a critical factor in their functionality[24]. According to the TEM micrographs, the size of the unloaded Cs/PAA nanogel was approximately 25 nm in the dried state. However, the DLS measurements revealed a significantly larger hydrodynamic radius of  $582.3 \pm 8.770$  nm, indicating substantial swelling of the nanogel in an aqueous environment. Similarly, for the berberine (BR)-loaded Cs/PAA nanogel, the TEM micrographs showed a particle size of approximately 55 nm, while the DLS measurements recorded a hydrodynamic radius of  $612.7 \pm 5.095$  nm.

The observed increase in particle size measured by DLS, compared to TEM, can be attributed to the hydration of the nanogel in aqueous solution. The polyacrylic acid (PAA) component of the nanogel absorbs water molecules, leading to swelling and an increase in the hydrodynamic radius. This phenomenon is consistent with the inherent hydrophilic nature of PAA, which facilitates water uptake and enhances the nanogel's swelling capacity[25].

Also, we can note that particle size from TEM after adding berberine to samples is approximately three times without berberine, while in DLS the numbers are very close to each other, Where The difference arises because TEM measures dry-state particle size, where berberine accumulation on the nanogel surface closes pores and increases apparent size, But in the case of DLS measures hydrodynamic diameter in distilled water, where both samples reach swelling equilibrium. The sample without berberine has higher porosity (thus greater swelling capacity), while the sample with berberine has reduced swelling due to surface loading, resulting in comparable hydrated sizes.

Additionally, the polydispersity index (PDI) values for the unloaded and BR-loaded nanogels were  $0.468 \pm 0.046$  and  $0.486 \pm 0.051$ , respectively, indicating a moderate size distribution. The zeta potential measurements, which reflect the surface charge and stability of the nanoparticles, were  $-13.3 \pm 2.72$  mV for the unloaded nanogel and  $-8.15 \pm 3.39$  mV for the BR-loaded nanogel, but the increasing value of error bars reflects sample

heterogeneity due to berberine's uneven distribution on the nanogel surface [26]. The negative zeta potential values suggest electrostatic stabilization of nanogels, which is essential for preventing aggregation and ensuring colloidal stability in aqueous media [27].

These findings highlight the significant influence of hydration on the size and stability of Cs/PAA nanogels, as well as their potential for applications in drug delivery systems, where controlled swelling and stability are critical for optimal performance.

**Table 1 Results of Particle size, Polydispersity index (PDI), and zeta potential using DLS technique.**

	Particle size (nm)	PDI	Zeta Potential (mv)
Cs/PAA nanogel	582.3 ± 8.770	0.468 ± 0.046	-13.3 ± 1.72
Cs/PAA nanogel loaded BR	612.7 ± 5.095	0.486 ± 0.051	-8.15 ± 1.39

### Thermogravimetric Analysis (TGA)

The thermal degradation behavior of chitosan-grafted polyacrylic acid (Cs-PAA) nanogel was investigated using thermogravimetric analysis (TGA). As illustrated in Figure (2a), the TGA curve reveals a multi-stage degradation process. The initial weight loss, observed between 30 °C and 135 °C, corresponds to the evaporation of residual or physically adsorbed water from the nanogel surface. The second stage, occurring between 134 °C and 192 °C, is attributed to the decomposition of phthalic anhydride groups. The third stage, spanning from 192 °C to 308 °C, involves the cleavage of C-O-C bonds within the chitosan backbone[28]. The fourth stage, between 308 °C and 477.8 °C, is associated with the degradation of carboxylic acid groups. Finally, the fifth stage, from 474 °C to 557 °C, represents the thermal decomposition of the chitosan structure [29]. The TGA results indicate relatively low thermal stability for the Cs-PAA nanogel, which is consistent with the presence of thermally labile functional groups in its structure[30].

Similarly, the thermal degradation of berberine (BR)-loaded chitosan/polyacrylic acid (Cs/PAA) nanogel was analyzed using TGA, as shown in Figure (2b). The initial weight loss, observed between 25.8 °C and 154.5 °C, is attributed to the loss of residual or physically adsorbed water from the nanogel surface [31]. The second stage, from 154.5 °C to 260 °C, corresponds to the decomposition of phthalic anhydride groups and the onset of berberine degradation, as the melting temperature of BR typically ranges between 109 °C and 188 °C [32]. The third stage, between 260 °C and 350 °C, involves the breakdown of C-O-C bonds in the chitosan backbone. The fourth stage, from 350 °C to 520 °C, is associated with the degradation of carboxylic acid groups, the decomposition of the chitosan structure, and the destruction of the BR skeleton[33].

These findings highlight the thermal behavior of both unloaded and BR-loaded Cs/PAA nanogels, providing valuable insights into their stability and degradation mechanisms. The incorporation of berberine appears to influence the thermal degradation profile, particularly in the higher temperature ranges, where the decomposition of BR and its interaction with the nanogel matrix become evident.

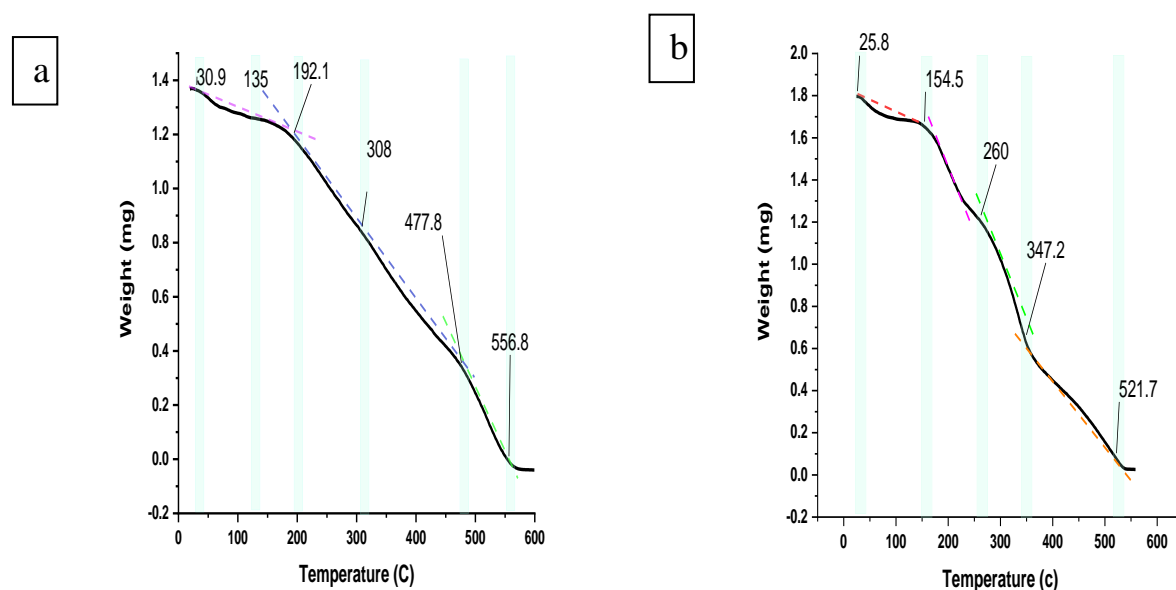


**Fig. 2 Thermogravimetric analysis (TGA) for (a) Cs/PAA nanogel without BR, (b) Cs/PAA nanogel loading BR.**

### In Vitro Cell Viability Assessment

The cytotoxicity and biocompatibility of chitosan/polyacrylic acid (Cs/PAA) nanogels, both unloaded and loaded with berberine (BR), were evaluated using the Sulforhodamine B (SRB) assay. Fibroblast cells were treated with varying concentrations (0.02–200  $\mu\text{L/mL}$ ) of Cs/PAA nanogel without BR and Cs/PAA nanogel loaded with BR for 24 hours. The results, as summarized in Table 2, demonstrate that the Cs/PAA nanogel loaded with BR exhibited significantly higher cell viability compared to the unloaded nanogel, particularly at higher concentrations[34].

At a concentration of 20  $\mu\text{L/mL}$ , the cell viability for Cs/PAA without BR was  $91.37 \pm 1.34\%$ , whereas for Cs/PAA loaded with BR, it was  $97.34 \pm 1.41\%$ . Similarly, at 200  $\mu\text{L/mL}$ , the cell viability for Cs/PAA without BR was  $90.94 \pm 2.38\%$ , while for Cs/PAA loaded with BR, it was  $95.75 \pm 0.82\%$ . These findings indicate that the incorporation of berberine into the Cs/PAA nanogel enhances its biocompatibility, as evidenced by the higher cell viability percentages[35].

The improved cell viability observed with BR-loaded nanogels suggests that berberine not only mitigates potential cytotoxic effects but also contributes to the bioactivity of the nanogel. This property is particularly advantageous for applications in skin wound healing, where maintaining high cell viability and promoting cellular proliferation are critical for effective tissue regeneration.

**Table 2 Cell viability assay showing the cytotoxic effects of (a) Cs/PAA nanogel without BR, (b) Cs/PAA nanogel loading BR on fibroblast cells.**

Cs/PAA	Raw data			Blank Corrected Data			Viability %				
Conc	1	2	3	1	2	3	1	2	3	Mean	STD
c	2.9443	2.9585	2.9514	2.9173	2.9315	2.9244	100	100	100	100	0
0.02	2.722	2.8372	2.896	2.695	2.8102	2.869	92.1557	96.0949	98.1056	95.4521	2.471221
0.2	2.6949	2.6644	2.9038	2.6679	2.6374	2.8768	91.229	90.186	98.3723	93.2624	3.638231
2	2.731	2.8102	2.8365	2.704	2.7832	2.8095	92.4634	95.1717	96.071	94.5687	1.533261
20	2.7133	2.6458	2.7384	2.6863	2.6188	2.7114	91.8582	89.55	92.7165	91.3749	1.337110
200	2.7029	2.5942	2.7626	2.6759	2.5672	2.7356	91.5025	87.7855	93.544	90.944	2.383818
Blank	0.0286	0.0266	0.0258	Blank Average		0.027	Control average		2.9244		

BR/Cs/PA	Raw data			Blank Corrected Data			Viability %				
Conc	1	2	3	1	2	3	1	2	3	Mean	STD
c	2.7367	2.7636	2.7114	2.7076	2.7345	2.6823	100	100	100	100	0
0.02	2.7095	2.7904	2.7014	2.6804	2.7613	2.6723	98.9759	101.963	98.6768	99.872	1.483756
0.2	2.7251	2.7149	2.6607	2.696	2.6858	2.6316	99.552	99.1753	97.1739	98.6337	1.043624
2	2.6521	2.715	2.6995	2.623	2.6859	2.6704	96.8564	99.179	98.6067	98.214	0.988022
20	2.7151	2.6588	2.6221	2.686	2.6297	2.593	99.1827	97.1038	95.7486	97.345	1.412305
200	2.6525	2.5995	2.6142	2.6234	2.5704	2.5851	96.8712	94.9141	95.4569	95.7474	0.824949
Blank	0.0277	0.0287	0.0309	Blank Average		0.0291	Control average		2.70813		

### Conclusion

This study successfully investigated the biophysical and biochemical properties of chitosan/polyacrylic acid (Cs/PAA) nanogels loaded with Berberine (BR) for potential biomedical applications, particularly in wound healing. The nanogels were synthesized using gamma irradiation, a technique that facilitated the polymerization and grafting of polyacrylic acid onto chitosan, resulting in a stable and uniform nanogel matrix. Advanced characterization techniques, including Transmission Electron Microscopy (TEM), Dynamic Light Scattering (DLS), Zeta Potential analysis, and Thermogravimetric Analysis (TGA), were employed to evaluate the morphological, structural, and thermal properties of the nanogels.

The TEM analysis revealed that both unloaded and BR-loaded nanogels exhibited spherical morphologies with smooth surfaces, with particle sizes of approximately 25 nm and 60 nm, respectively. The DLS measurements indicated significant swelling in aqueous environments, with hydrodynamic radii of  $582.3 \pm 8.770\text{nm}$  for unloaded nanogels and  $612.7 \pm 5.095\text{ nm}$  for BR-loaded nanogels. The zeta potential values confirmed the colloidal stability of the nanogels, with negative surface charges preventing aggregation. TGA results demonstrated the thermal degradation profiles of the nanogels, highlighting the influence of berberine on their thermal stability.

In vitro cell viability assessments using the Sulforhodamine B (SRB) assay demonstrated that the BR-loaded nanogels exhibited significantly higher biocompatibility compared to unloaded nanogels, with cell viability percentages of  $97.34 \pm 1.41\%$  and  $95.75 \pm 0.82\%$  at concentrations of 20  $\mu\text{L/mL}$  and 200  $\mu\text{L/mL}$ , respectively.

These findings underscore the enhanced bioactivity and reduced cytotoxicity of the BR-loaded nanogels, making them a promising candidate for wound healing applications.

The incorporation of berberine into the Cs/PAA nanogel matrix not only improved its therapeutic efficacy but also addressed the limitations of berberine's poor bioavailability. The nanogel's ability to provide sustained release, enhance cellular uptake, and promote wound healing was evident from the experimental results. Overall, this study highlights the potential of BR-loaded Cs/PAA nanogels as a novel and effective therapeutic strategy for skin wound healing, offering a combination of biocompatibility, controlled drug delivery, and enhanced therapeutic outcomes. Future research should focus on in vivo studies to further validate the efficacy and safety of this innovative formulation in clinical applications.

### Conflicts of interest:

The authors declare that there is no conflict of interest regarding the publication of this article.

### References

1. **Dekoninck, S. and Blanpain, C.** Stem cell dynamics, migration and plasticity during wound healing. *Nature Cell Biology*, **21** (1), 18-24 (2019). doi:10.1038/s41556-018-0237-6.
2. **Ghani, A., Zare, E.N., Makvandi, P. and Rabiee, N.** Antioxidant, antibacterial and biodegradable hydrogel films from carboxymethyl tragacanth gum and clove extract: Potential for wound dressings application. *Carbohydrate Polymer Technologies and Applications*, **7**, 100428 (2024). doi:10.1016/j.carpta.2024.100428.
3. **Jabeen, N. and Atif, M.** Polysaccharides based biopolymers for biomedical applications: A review. *Polymer Advances Technology*, **35** (1), e6203 (2024). doi:10.1002/pat.6203.
4. **Jayaramudu, T., Varaprasad, K., Reddy, K.K., Pyarasani, R.D., Akbari-Fakhrabadi, A. and Amalraj, J.** Chitosan-pluronic based Cu nanocomposite hydrogels for prototype antimicrobial applications. *International Journal of Biological Macromolecules*, **143**, 825-832 (2020). doi:10.1016/j.ijbiomac.2019.09.143.
5. **Karg, M., et al.** Nanogels and Microgels: From Model Colloids to Applications, Recent Developments, and Future Trends. *Langmuir*, **35** (19), 6231-6255 (2019). doi:10.1021/acs.langmuir.8b04304.
6. **Schexnailder, P. and Schmidt, G.** Nanocomposite polymer hydrogels. *Colloid and Polymer Science*, **287** (1), 1-11 (2009). doi:10.1007/s00396-008-1949-0.
7. **González-Ayón, M.A., Licea-Claverie, A. and Sañudo-Barajas, J.A.** Different strategies for the preparation of galactose-functionalized thermo-responsive nanogels with potential as smart drug delivery systems. *Polymers*, **12** (9), (2020). doi:10.3390/polym12092150.
8. **Sanson, N. and Rieger, J.** Synthesis of nanogels/microgels by conventional and controlled radical crosslinking copolymerization. *Polymer Chemistry*, (2010). doi:10.1039/c0py00010h.
9. **Wang, B., Mukataka, S., Kokufuta, E. and Kodama, M.** The influence of polymer concentration on the radiation-chemical yield of intermolecular crosslinking of poly(vinyl alcohol) by  $\gamma$ -rays in deoxygenated aqueous solution. *Radiation Physics and Chemistry*, **59** (1), 91-95 (2000). doi:10.1016/S0969-806X(00)00188-2.
10. **Ashfaq, A., et al.** Polymerization Reactions and Modifications of Polymers by Ionizing Radiation. *Polymers*, **12** (12), 2877 (2020). doi:10.3390/polym12122877.
11. **Rouif, S.** Radiation cross-linked polymers: Recent developments and new applications. *Nuclear Instruments and Methods in Physics Research Section B: Beam Interactions with Materials and Atoms*, **236** (1-4), 68-72 (2005). doi:10.1016/j.nimb.2005.03.252.
12. **Mikušová, V. and Mikuš, P.** Advances in Chitosan-Based Nanoparticles for Drug Delivery. *International Journal of Molecular Sciences*, **22** (17), (2021). doi:10.3390/ijms22179652.
13. **Arkaban, H., et al.** Polyacrylic Acid Nanoplateforms: Antimicrobial, Tissue Engineering, and Cancer Theranostic Applications. *Polymers*, **14** (6), 1259 (2022). doi:10.3390/polym14061259.
14. **Khan, S., et al.** A review of the berberine natural polysaccharide nanostructures as potential anticancer and antibacterial agents. *Biomedicine & Pharmacotherapy*, **146**, 112531 (2022). doi:10.1016/j.biopha.2021.112531.
15. **Wojtyczka, R.D., et al.** Berberine Enhances the Antibacterial Activity of Selected Antibiotics against Coagulase-Negative Staphylococcus Strains in Vitro. *Molecules*, **19** (5), 6583 (2014). doi:10.3390/molecules19056583.
16. **Xu, X., et al.** Therapeutic effect of berberine on metabolic diseases: Both pharmacological data and clinical evidence. *Biomedicine & Pharmacotherapy*, **133**, 110984 (2021). doi:10.1016/j.biopha.2020.110984.
17. **Gholampour, F. and Keikha, S.** Berberine protects the liver and kidney against functional disorders and histological damages induced by ferrous sulfate. *Iranian Journal of Basic Medical Sciences*, **21** (5), 476-482 (2018). doi:10.22038/ijbms.2018.25199.6241.
18. **Tong, J., et al.** A berberine hydrochloride-carboxymethyl chitosan hydrogel protects against Staphylococcus aureus infection in a rat mastitis model. *Carbohydrate Polymers*, **278**, 118910 (2022). doi:10.1016/j.carbpol.2021.118910.

19. **Radwan, R.R., Abdel Ghaffar, A.M. and Ali, H.E.** Gamma radiation preparation of chitosan nanoparticles for controlled delivery of memantine. *Journal of Biomaterials Applications*, **34** (8), 1150-1162 (2020). doi:10.1177/0885328219890071.
20. **Radwan, R.R. and Ali, H.E.** Radiation-synthesis of chitosan/poly (acrylic acid) nanogel for improving the antitumor potential of rutin in hepatocellular carcinoma. *Drug Delivery and Translational Research*, **11** (1), 261-278 (2021). doi:10.1007/s13346-020-00792-7.
21. **Hu, Y., Chen, Y., Chen, Q., Zhang, L., Jiang, X. and Yang, C.** Synthesis and stimuli-responsive properties of chitosan/poly(acrylic acid) hollow nanospheres. *Polymer*, **46** (26), 12703-12710 (2005). doi:10.1016/j.polymer.2005.10.110.
22. **Radwan, R.R., Abdel Ghaffar, A.M. and Ali, H.E.** Gamma radiation preparation of chitosan nanoparticles for controlled delivery of memantine. *Journal of Biomaterials Applications*, **34** (8), 1150-1162 (2020). doi:10.1177/0885328219890071.
23. **Mehra, M., et al.** Synthesis and evaluation of berberine loaded chitosan nanocarrier for enhanced in-vitro antioxidant and anti-inflammatory potential. *Carbohydrate Polymer Technologies and Applications*, **7**, 100474 (2024). doi:10.1016/j.carpta.2024.100474.
24. **Gungor Ak, A., Turan, I., Sayan Ozacmak, H. and Karatas, A.** Chitosan nanoparticles as promising tool for berberine delivery: Formulation, characterization and in vivo evaluation. *Journal of Drug Delivery Science and Technology*, **80**, 104203 (2023). doi:10.1016/j.jddst.2023.104203.
25. **Ghobadi-Oghaz, N., Asoodeh, A. and Mohammadi, M.** Fabrication, characterization and in vitro cell exposure study of zein-chitosan nanoparticles for co-delivery of curcumin and berberine. *International Journal of Biological Macromolecules*, **204**, 576-586 (2022). doi:10.1016/j.ijbiomac.2022.02.041.
26. **Gungor Ak, A., Turan, I., Sayan Ozacmak, H. and Karatas, A.** Chitosan nanoparticles as promising tool for berberine delivery: Formulation, characterization and in vivo evaluation. *Journal of Drug Delivery Science and Technology*, **80**, 104203 (2023). doi:10.1016/j.jddst.2023.104203.
27. **Akhter, M.H., et al.** Enhanced drug delivery and wound healing potential of berberine-loaded chitosan-alginate nanocomposite gel: characterization and in vivo assessment. *Frontiers in Public Health*, **11**, 1238961 (2023). doi:10.3389/fpubh.2023.1238961.
28. **Chuang, C.Y., Don, T.M. and Chiu, W.Y.** Synthesis and properties of chitosan-modified poly(acrylic acid). *Journal of Applied Polymer Science*, **109** (5), 3382-3389 (2008). doi:10.1002/app.28420.
29. **Guo, L., Liu, G., Hong, R.Y. and Li, H.Z.** Preparation and Characterization of Chitosan Poly(acrylic acid) Magnetic Microspheres. *Marine Drugs*, **8** (7), 2212-2222 (2010). doi:10.3390/md8072212.
30. **Zhang, Y., et al.** Bilayer Membrane Composed of Mineralized Collagen and Chitosan Cast Film Coated With Berberine-Loaded PCL/PVP Electrospun Nanofiber Promotes Bone Regeneration. *Frontiers in Bioengineering and Biotechnology*, **9**, 684335 (2021). doi:10.3389/fbioe.2021.684335.
31. **Rahman, M.M., Lata, N.N., Rimu, S.H. and Chisty, A.H.** Simultaneous determination of heavy metals and cationic dyes from industrial effluent by prawn shell derived chitosan-g-poly(acrylic acid) biocomposite. *Desalination and Water Treatment*, **216**, 252-262 (2021). doi:10.5004/dwt.2021.26859.
32. **Moniot, J.L. and Shamma, M.** Conversion of Berberine into Phthalideisoquinolines. *Journal of Organic Chemistry*, **44** (24), 4337-4342 (1979). doi:10.1021/jo01338a020.
33. **Wahab, S., et al.** Hydrogel: An Encouraging Nanocarrier System for the Delivery of Herbal Bioactive Compounds. *Current Nanoscience*, **17** (6), 797-807 (2021). doi:10.2174/1573413717666210216161701.
34. **Khan, M.J., Hafeez, A. and Siddiqui, M.A.** Nanocarrier Based Delivery of Berberine: A Critical Review on Pharmaceutical and Preclinical Characteristics of the Bioactive. *Current Pharmaceutical Biotechnology*, **24** (11), 1449-1464 (2023). doi:10.2174/1389201024666230112141330.
35. **Dehchani, A.J., Jafari, A. and Shahi, F.** Nanogels in Biomedical Engineering: Revolutionizing Drug Delivery, Tissue Engineering, and Bioimaging. *Polymer Advances Technology*, **35** (10), e6595 (2024). doi:10.1002/pat.6595.

## تقييم الخصائص الفيزيائية الحيوية والكيميائية الحيوية للهلام النانو جل ( كيتوزان / حمض البولي اكرليك ) المحل بالبربرين ل استخدامه في التطبيقات الطبية الحيوية

محمد إبراهيم ملجي<sup>1\*</sup>، محمود حسن عبد الجواد<sup>1</sup>، شيماء ناصف<sup>2</sup>، هاني البهنساوي<sup>1</sup>

<sup>1</sup> قسم الفيزياء، شعبة الفيزياء الحيوية، كلية العلوم (بنين)، جامعة الأزهر؛ <sup>2</sup> قسم كيمياء البوليمرات، المركز القومي لبحوث وتكنولوجيا الإشعاع، الهيئة المصرية للطاقة الذرية.

الهدف من الدراسة هو تقييم الخصائص الفيزيائية الحيوية والكيميائية الحيوية للهلام النانو جل ( كيتوزان / حمض البولي اكرليك ) المحل بالبربرين ل استخدامه في التطبيقات الطبية الحيوية خاصة في مجال التئام الجروح عن طريق تصنيع هلامات النانو باستخدام تقنية الإشعاع الجامي، وهي طريقة سهلت عملية البلمرة وتركيب حمض البولي اكرليك على الكيتوزان، مما أدى إلى تكوين مصفوفة نانوية مستقرة وموحدة .

المواد والطرق : تم استخدام تقنيات متقدمة مثل الفحص المجهر الإلكتروني النافذ (TEM) ، وتشتت الضوء الديناميكي (DLS) ، وتحليل جهد زيتا، والتحليل الحراري الوزني (TGA) لتقييم الخصائص الشكلية والهيكلية والحرارية لهلامات النانو. النتائج والمناقشة : كشف تحليل TEM أن هلامات النانو غير المحملة والمحملة بالبربرين تتمتع بشكل كروي مع أسطح ملساء، بأحجام جسيمات تبلغ حوالي 25 نانومتر و 60 نانومتر على التوالي. أشارت قياسات DLS إلى تورم كبير في البيئات المائية، مع أنصاف أقطار هيدروديناميكية تبلغ  $582.3 \pm 8.770$  نانومتر للهلامات غير المحملة و  $612.7 \pm 5.095$  نانومتر للهلامات المحملة بالبربرين. أكدت قيم جهد زيتا استقرار الهلامات الغروية، مع شحنات سطحية سالبة تمنع التكتل. أظهرت نتائج TGA سلوك التحلل الحراري للهلامات، مع إبراز تأثير البربرين على ثباتها الحراري.

أظهرت تقييمات حيوية الخلايا باستخدام اختبار Sulforhodamine B (SRB) أن الهلامات المحملة بالبربرين تتمتع بدرجة أعلى من التوافق الحيوي مقارنة بالهلامات غير المحملة، مع نسب حيوية للخلايا تبلغ  $97.34 \pm 1.41\%$  و  $95.75 \pm 0.82\%$  عند تركيزات 20 ميكرو لتر/مل و 200 ميكرو لتر/مل على التوالي.

هذه النتائج تؤكد النشاط الحيوي المحسن والسمية الخلوية المنخفضة للهلامات المحملة بالبربرين، مما يجعلها مرشحة وإعادة لتطبيقات التئام الجروح.

الاستنتاج : إن دمج البربرين في مصفوفة هلامات النانو لم يحسن فقط من فعاليتها العلاجية، بل أيضًا عالج قيود النوافر الحيوي الضعيف للبربرين. كانت قدرة الهلامات على توفير إطلاق مستدام، وتعزيز امتصاص الخلايا، وتعزيز التئام الجروح واضحة من النتائج التجريبية. بشكل عام، تسلط هذه الدراسة الضوء على إمكانات هلامات النانو المحملة بالبربرين كاستراتيجية علاجية مبتكرة وفعالة لالتئام جروح الجلد، حيث توفر مزيجًا من التوافق الحيوي، التحكم في إطلاق الدواء، وتحسين النتائج العلاجية. يجب أن تركز الأبحاث المستقبلية على الدراسات السريرية لتأكيد فعالية وسلامة هذا التركيب المبتكر في التطبيقات السريرية .